The Antithrombogenic Potential of a Polyhedral Oligomeric Silsesquioxane (POSS) Nanocomposite

Ruben Y. Kannan,[†,‡] Henryk J. Salacinski,[†,§] Jaco De Groot,[∥] Ian Clatworthy,[#] Laurent Bozec,[⊥] Mike Horton,[⊥] Peter E. Butler,[‡] and Alexander M. Seifalian*[,†,§]

Biomaterials & Tissue Engineering Centre (BTEC), Academic Division of Surgical and Interventional Sciences, University College London, Department of Plastic Surgery, Royal Free Hampstead NHS Trust, London, U.K., Advanced Nanomaterials laboratory (ANL), BTEC, University College London, Birkbeck College, School of Biological and Chemical Sciences Birkbeck College, University of London, London Centre for Nanotechnology and Department of Medicine, University College London, and Electron Microscopy Unit, Royal Free University College Medical School, London, U.K.

Received August 18, 2005; Revised Manuscript Received October 9, 2005

We have developed a nanocomposite using a silica nanocomposite polyhedral oligomeric silsesquioxane (POSS) and poly(carbonate−urea)urethane (PCU) for potential use in cardiovascular bypass grafts and the microvascular component of artificial capillary beds. In this study, we sought to compare its antithrombogenicity to that of conventional polymers used in vascular bypass grafts so as to improve upon current patency rates, particularly in the microvascular setting. Using atomic force microscopy (AFM) and transmission electron microscopy (TEM), surface topography and composition were studied, respectively. The ability of the nanocomposite surface to repel both proteins and platelets in vitro was assessed using thromboelastography (TEG), fibrinogen ELISA assays, antifactor Xa assays, scanning electron microscopy (SEM), and platelet adsorption tests. TEG analysis showed a significant decrease in clot strength (one-way ANOVA, $p < 0.001$) and increase in clot lysis (one-way ANOVA, $p < 0.0001$) on the nanocomposite when compared to both poly(tetrafluoroethylene) (PTFE) and PCU. ELISA assays indicate lower adsorption of fibrinogen to the nanocomposite compared to PTFE (one-way ANOVA, $p < 0.01$). Interestingly, increasing the concentration of POSS nanocages within these polymers was shown to proportionately inhibit factor X activity. Platelet adsorption at 120 min was also lower compared to PTFE and PCU (two-way ANOVA, $p < 0.05$). SEM images showed a "speckled" morphologic pattern with Cooper grades I platelet adsorption morphology on the nanocomposite compared to PTFE with grade IV morphology. On the basis of these results, we concluded that POSS nanocomposites possess greater thromboresistance than PTFE and PCU, making it an ideal material for the construction of both bypass grafts and microvessels.

Introduction

The ideal cardiovascular graft, whether a bypass graft or a microvessel, should have the ability to withstand high shear stresses, have similar bulk viscoelasticity to those of the native vessels they are anastomosed to, and, most importantly, possess thromboresistant properties. With decreasing vessel diameters at low-flow states,[1] the interplay between these factors is significantly amplified. While results with poly(tetrafluoroethylene) (PTFE) and poly(ethylene terephthalate) (Dacron) are satisfactory in larger vessels, patency is far lower in small-diameter grafts,[2] especially with Dacron, which has high platelet adsorption characteristics.[3] In the case of microvessels (<1 mm diameter), animal models using PTFE have shown a 20−25% patency rate in rat femoral vessels, while the control vein grafts in the experiment remained patent.[4] This is because these polymers adsorb significant amounts of fibrinogen[5] and activate thrombus formation on its lumen,[6] while the differential compliance at the anastomotic site causes the formation of intimal hyperplasia (IH).[7−9]

Therefore, autologous vein grafts remain the "gold standard" for both macro- and microvascular repairs[2] at low-flow states, as they are both compliant and nonthrombogenic. However, donor-site morbidity and the need for an additional surgery remain the drawbacks. To overcome this, there has been considerable work put into developing biological alternatives, particularly as small-diameter and microvascular grafts.[10] Their main advantages include non-thrombogenicity and optimal radial compliance, but growing them in vitro is lengthy with a high possibility of infection.[1,2,10,11] This has prompted other researchers to look into ready-made polymeric options which are bioactive or, in other words, mimic the biology of nature's vessels. While PTFE and Dacron have limitations, certain groups have turned to polyurethanes (PU), as they possess optimal physicomechanical properties and are resistant to flexural fatigue.[12] We have previously worked on a newer carbonate-based polyurethane, poly(carbonate−urea)urethane (PCU), which

* Corresponding author Alexander M. Seifalian, M.Sc., P.G.Dip., Ph.D., F.Int.Nano., Professor of Biophysics & Tissue Engineering & Director of BTEC, Biomaterials & Tissue Engineering Centre (BTEC), University College London (UCL), Rowland Hill, Hampstead, London NW3 2PF, U.K. Tel: ++44 20 7830 2901 (direct). Fax: ++44 20 7472 6444. Email: A.Seifalian@UCL.AC.UK.

[†] Biomaterials & Tissue Engineering Centre (BTEC), Academic Division of Surgical and Interventional Sciences, University College London.

[‡] Department of Plastic Surgery, Royal Free Hampstead NHS Trust.

[§] Advanced Nanomaterials laboratory (ANL), BTEC, University College London.

[∥] Birkbeck College, School of Biological and Chemical Sciences Birkbeck College, University of London.

[⊥] London Centre for Nanotechnology and Department of Medicine, University College London.

[#] Electron Microscopy Unit, Royal Free University College Medical School.

10.1021/bm050590z CCC: $33.50
Published on Web 11/15/2005

has been shown to have superior resistance to both hydrolytic and oxidative degradation[13] as well as similar viscoelasticity characteristics to those of biological vessels as determined in an in vitro pulsatile flow circuit.[9] After implantation of PCU bypass grafts in a canine model for 36 months, they retained their elasticity and mechanical properties, which indicates optimal biostability.[14] The graft has been marketed for dialysis bypass as a short-term application. In long-term implantation, even these polymers only have moderate haemocompatibility, which needs to be improved upon before use as small-diameter and microvessels.

As such, efforts are currently being made to improve upon the surface haemocompatibility of conventional polymers.[15] Studies by Silver and colleagues revealed that the haemocompatibility of a surface depends on the wettability characteristics of its surface.[16] Therefore, incorporating silicon, which repels platelet and fibrin adsorption because of its variable surface tension, onto a vascular interface would confer to it increased thromboresistance.[17] A disadvantage of silicon-containing vessels, however, is that they are rigid and would have minimal radial elasticity with a tendency to form intimal hyperplasia more rapidly. Further studies have also revealed that shorter and more mobile surface moieties have increased thromboresistance,[17,18] thus strengthening the need for the use of nanoparticles. Our original hypothesis was to use silsesquioxanes (SQS), which contain silicon, to produce thromboresistant vessels that still retain viscoelastic properties.[19]

Previously, we developed and assessed the cytocompatibility of a new nanocomposite based on polyurethane and bridge monomers of SQS.[20] Herein, we have moved this work significantly further on by using these building-block monomers to construct cage-type structures.[21] Our original hypothesis is that this approach at nanocores will confer significant antithrombogenic qualities previously not possible with the former approach[22] due to the surface closed-cage polyhedral oligomeric silsesquioxane (POSS) pendant chain in this nanocomposite. The POSS nanoparticle is composed of two cyclic rings composed of silicon and oxygen in accordance with the stoichometric formula $(SiO_{1.5})_8$.[19] Depending on the number of side groups, it may exist as pendant cages, be part of a polymeric backbone, or be cross-linked. Researchers have since shown that these nanocomposite cubes may be incorporated as building-block fillers or cores into other polymers to form hybrid inorganic−organic copolymers with improved miscibility and hence elasticity.[23] In addition, optimal POSS dispersion within the polymer serves as reinforcing nanofiller with high surface coverage. We have shown that POSS cages also possess optimal cytocompatibility.[24]

Prior studies have shown that POSS nanocomposites have the ability to self-assemble once mixed with other polymers.[25] On the basis of these data, we synthesized a nanocomposite using a modification of the POSS molecule; *trans*-cyclohexanediol isobutyl-POSS (Figure 1) chemically integrated with poly(carbonate−urea)urethane (PCU). This improves the surface mobility of the copolymer and hence potentially reduces the urethane group's functionality of both protein and platelet adsorption responsible for activating coagulation.[26] Our postulate is that a pendant nanocage containing silicon atoms would form foci of silicon-rich areas serving as the scaffold while allowing the polyurethane component to form the bulk of the polymer, hence maintaining its compliant properties. In vivo studies have shown that there is no inflammation or capsule formation indicative of antithrombogenicity.[27] In this set of in vitro experiments, we determined whether this polymer, POSS−PCU, has the aforementioned antithrombogenic properties and sought to understand the reasons for its behavior in this manner.

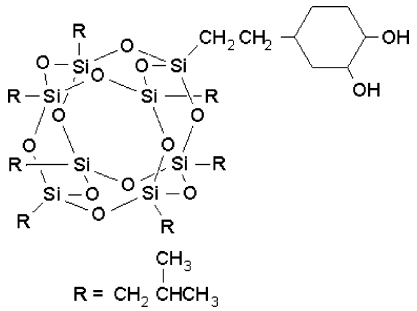

Figure 1. Molecular structure of *trans*-cyclohexanediol isobutyl-POSS. Molecular formula $C_{36}H_{78}O_{14}Si_8$.

Methods and Materials

Polymer Synthesis. Polycarbonate polyol and *trans*-cyclohexanediol isobutyl-POSS (Figure 1) were placed in a reaction flask equipped with a stirrer and nitrogen. The mixture was heated to 125 °C to dissolve the nanocage and then cooled to 60 °C. To this, methylene diisocyanate (MDI) was added and reacted at 70−80 °C for 90 min to form a prepolymer. Then, *N*,*N*-dimethylacetamide (DMAC) was added. Chain extension was carried out by the addition of ethylenediamine and diethylamine in DMAC. Then, 4 g of 1-butanol in dimethylacetamide was added to form a 2% polyhedral oligomeric silsesqioxane−poly(carbonate−urea)urethane (POSS−PCU) solution. By increasing the amount of *trans*-cyclohexanediol isobutyl-silsesquioxane used to 6 g, a corresponding 6% POSS−PCU solution was formed.[22] All chemicals and reagents were purchased from Aldrich Limited, Gillingham, U.K.

Characterization. Polymer samples for transmission electron microscopy (TEM) were prepared using thin slivers of 2% POSS−PCU, which were removed from the glass slide and placed in plastic molds that were then filled with Lemix epoxy resin and polymerized in an oven at 70 °C overnight. Sections (0.5 μm) were cut using a diamond knife (Diatome) on a Reichert−Jung ultracut microtome and collected on 200HS, 3.05-mm copper grids (Gilder) coated with Butvar support film. The sections were viewed and photographed at up to 53 000× magnification using a Philips CM120 transmission electron microscope at 80 kV to understand the composition of the polymer. The elemental composition of these regions were then analyzed using energy dispersion X-ray analysis (EDXA). X-ray spectra and maps were also acquired using an EDXA DX-4 EDS X-ray microanalysis system.

Using the sessile drop method, the contact angle of 2% POSS−PCU with reference to water was determined with a Rame−Hart contact angle goniometer.[28] HPLC-grade pure distilled water was introduced via a syringe to place droplets of water onto the surface of the polymer. Both advanced and receded contact angles were measured by increasing and decreasing the volume of the drop in 2 μL increments, respectively, in a similar fashion. Four independent measurements were performed on each sample ($n = 4$).

Atomic Force Microscopy. The surface topography of the 2% POSS−PCU nanocomposite and PCU was studied with a commercial atomic force microscope (Nanowizard, JPK Instruments, Berlin) using both contact and intermittent contact modes. For this purpose, the nanocomposite was prepared by casting it on new glass cover slips and left to dry at 70 °C for 72 h before being carefully peeled off using fine forceps and wrapped in aluminum foil to avoid surface contamination. Contact imaging was performed with a commercial AFM cantilever (gold-coated Microlevers, type C, Veeco Metrolgy Group, Sunnyvale, CA) at scan speeds of 1 Hz (Figure 4A) and 2.5 Hz (Figure 4B). Intermittent contact imaging was performed at a scan speed of 1 Hz with a commercial noncontact silicon cantilever (Ultrasharp, NSC12/50, type A, MikroMasch, Talinn, Estonia).

Thromboelastography. With a thromboelastograph (TEG) coagulation analyzer (TEG, Niles, IL), calibrated at 37 °C, 4.5 mL of blood was collected using the two-syringe technique in a citrated tube to constitute 3.8% citrated whole blood (CWB) at 1:10 v/v, pH 7.4.[29] The CWB is then gently inverted thrice to mix it and incubated for 15 min. In the meantime, 0.2 M calcium chloride was left to thaw at room temperature for 10 min. TEG cups were coated with a thin, uniform layer of 2% POSS−PCU in DMAC and incubated at 50 °C to remove DMAC. These cups were then mounted onto the TEG analyzer, and 20μL calcium chloride was added to each cup, followed by 340 μL of blood. The mixture was then coated with 6 drops of mineral oil to prevent blood evaporation and finally mixed by gently lowering and raising the pin.

Similarly, parallel analysis using poly(carbonate−urea)urethane (PCU) with empty polystyrene TEG cups as the control was performed in comparison to 2% POSS−PCU. Each of these tests was performed using blood from healthy volunteers ($n = 6$). TEG tests on PTFE were not done, as these high-extrusion polymers did not allow the casting of a thin, uniform layer on the cups. Any other method of coating the TEG cups with these polymers would have significantly altered the outcome and was hence not attempted. Tests on poly(ethylene terephthalate) (Dacron) were not performed in any of these experiments, as it is known that it is not the optimal material for smaller-diameter grafts and microvessels [4,30]

Fibrinogen Adsorption. Fibrinogen adsorption to POSS−PCU was determined using direct ELISA. The bases of 24-well polystyrene plates were coated with flat sheets of 2% POSS−PCU, PCU, and PTFE (Goretex, WL Gore Ltd., U.S.A.) with plain, uncoated polystyrene wells as controls. A quantity (100 μL) of 5% semiskimmed milk (Marvel) in PBS solution was then placed in each well for 2 h at 37 °C to block nonspecific antibody binding. This solution was removed and the wells rinsed with 0.01% Tween in PBS solution. A quantity (100 μL) of human fibrinogen solution (310 mg/mL) was then placed in each well and incubated at 37 °C for an hour to allow fibrinogen adsorption to the polymers. This was then carefully rinsed again and replaced with 100 μL of a 1:1600 rabbit antihuman fibrinogen HRP-tagged conjugated antibody (Dako Ltd., U.S.A.) in 2% serum bovine albumin for a further 2 h. This enzyme complex was then removed, and a solution of *ortho*-phenylamine diamine (ODP) in acid citrate buffer was then added to the wells and the color change allowed for 3 min before the reaction was terminated with 100 μL of 1% sulfuric acid. The wells were then exposed to an absorption spectrum of 490 nm to determine the readings (Dynex MRV, Prior Laboratory Supplies Ltd., U.K.). This experiment was performed with 4 repeats ($n = 4$). No experiments were performed on poly(ethylene terephthalate) for the reasons mentioned above.

Antifactor Xa Activity. Blood collected from healthy, normal volunteers without the use of tourniquets was citrated with 3.8% (w/v) trisodium citrate. The samples were then centrifuged at 250 g for 10 min and then recentrifuged at 13 000 g for 30 s using a microcentrifuge. This was followed by snap-freezing 250-mL aliquots of the plasma in liquid nitrogen before being stored at −80 °C. Prior to thrombogenicity analysis, these aliquots of platelet-poor plasma (PPP) were prewarmed at 37 °C.[31]

The antifactor Xa activity[32] of 2% and 6% POSS−PCU was studied using a factor X assay kit (AMAX ACCUCOLOR kit, Trinity Biotech, U.S.A.) with plain PCU and PTFE (Goretex Ltd., U.S.A.) as the controls. The bases of 0.28-cm^2 well plates were sealed with solid, flat sheets of POSS−PCU, PCU, and PTFE. Heparin standards were prepared by diluting heparin in PPP to form decreasing concentrations of 1.0, 0.5, 0.25, and 0.125 IU/mL, constituting the heparin reference standard. The heparin solutions and PPP were diluted 1:2 in PBS to be used in the control and sample groups, respectively. To this, 75 μL of human antithrombin III was initially added to each well, followed by 25 μL of the 1:2 heparin solutions, in the case of the control, and PPP, in the case of the sample. This was allowed to incubate for 2 min at 37 °C before adding another 75 μL of bovine factor Xa and incubating it 1 min further in the same setting. Next, 75 μL of factor Xa substrate (MeO-CO-D-CHG-Gly-Arg-pNA) was added and reincubated for 10 min at 37 °C. Activated factor X (FXa) hydrolyzed this substrate to release the chromophobe, *para*-nitroanilide (pNA). Thus, the amount of pNA released is inversely proportional to the extent of factor Xa inactivation. The reaction was terminated by the addition of 75 μL of glacial acetic acid. Then, 100 μL of this mixture was analyzed at the 420-nm absorption band to detect pNA and compared to the blank reagent. The latter was prepared in the same manner except that the wells were filled with acetic acid first. The antifactor Xa property of POSS−PCU was expressed as heparin equivalents per unit area (IU per cm^2). All experiments were repeated 6 times and in duplicate ($n = 6$).

Platelet Adhesion. The bases of 24-well polystyrene plates were sealed with flat sheets of the polymer and then hydrated in PBS for 24 h. Next, 1.0 mL of platelet-rich precipitate (PRP) at a concentration of 1.3×10^6 platelets/μL was added and incubated at 37 °C for 30, 60, and 120 min in a shaker. The PRP was then removed, and each container was then rinsed with PBS. The extract was counted immediately in a Coulter counter. PRP were also incubated in wells with PCU and PTFE, while uncoated polystyrene wells were used as controls. The number of platelets attached to POSS−PCU was calculated from the difference between the number of platelets in the PRP control and those left in the extract. The quantitative analysis of platelets attaching to POSS−PCU was expressed using Salzman's platelet retention index (PRI)[33] as shown below

$$\mathrm{PRI}\ (\%) = 100(\mathrm{PLTi} - \mathrm{PLTe})/\mathrm{PLTi}$$

where PLTi represents the concentration of the platelet precipitate prior to adsorption and PLTe represents its concentration after adsorption.

Platelet adsorption morphology was analyzed using scanning EM (SEM). First, 20 × 20 mm^2 glass slides coated with POSS−PCU and PTFE ($n = 6$) were placed in polystyrene containers filled with 2 mL of PRP at a density of 3×10^5 cells/mL at 37 °C. After rinsing with PBS and fixing with glutaraldehyde solution (2.5 v/v %) in PBS for 2 h at room temperature, the samples were dehydrated with ethanol/distilled water (10% ethanol increments) at 41 °C. This was followed by freeze-drying for 48 h before subjecting them to SEM observation.

Results

POSS Nanocage Distribution. TEM analysis on cast polymer sheets revealed that the darker areas of the nanocomposite correspond to the crystalline hard segment of the nanocomposite, whereas the amorphous soft segment was optically less dense. EDXA mapping on these samples showed three specific regions; yellow silicon and oxygen-rich POSS segment(s) immediately surrounded by light purple areas of urethane, which together constitute the hard segment, and a dark purple area corresponding to the carbon-rich carbonate soft segment (Figure 2A). TEM also showed that the silicon-rich POSS regions were distributed evenly throughout the hard segments of the nanocomposite, while the presence of yellow speckled dots (silicon) within the amorphous domain also suggested POSS incorporation into the soft segment at the nanoscale. These POSS groups residing within the hard segment of PCU extended into the soft segment to form nebulous patterns as shown in Figure 2B, indicating an exfoliated type of nanocomposite.[19] This shows that POSS nanocages act as cross-linkers, which form a 3-D netlike internal scaffold within the existing structural framework of the polyurethane hard segment,[19,34] binding together the remaining constituents not unlike a "wire mesh".

Water Contact Angle Measurement. POSS−PCU (2%) had an advanced contact angle of 81 ± 2° and a receded angle of 36 ± 5°, which reveals a large difference between the advanced and receded angles (contact angle hysteresis; Figure 3) compared

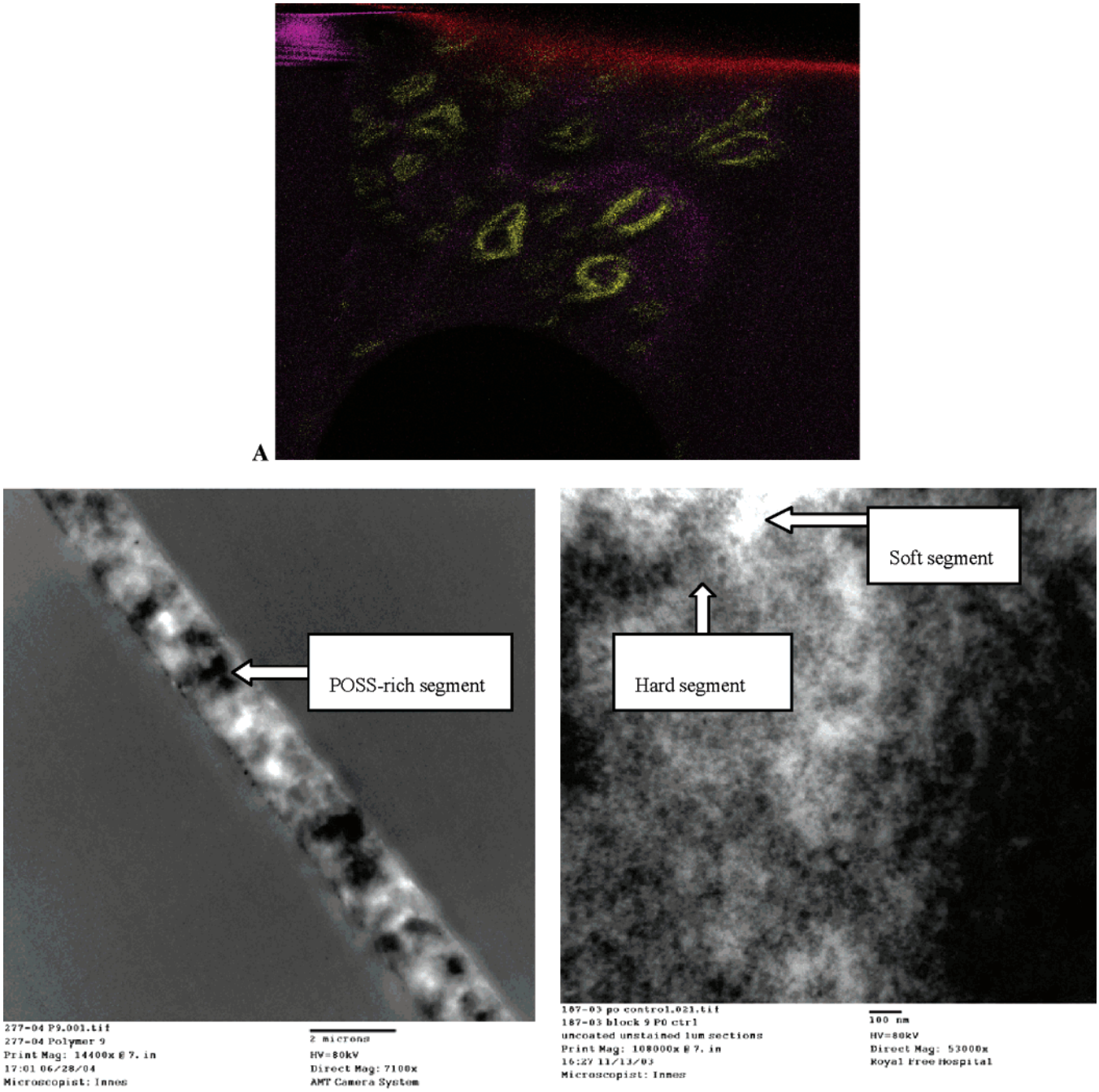

Figure 2. (A) EDXA map of 2% POSS−PCU showing the distribution of POSS (yellow) within the hard segment of the polymer (light purple), while softer segments correlate to purple areas of carbon. The red line represents the copper grid. On closer inspection, speckled yellow dots may also be seen within the soft (purple) segments of the polymer, indicating that POSS molecules also interact with the amorphous carbonate segment. (B) TEM analysis of a cross-section of 2% POSS−PCU cast sheets showing the distribution of silicon-rich POSS segments within the darker, hard segments of the nanocomposite while gradually encroaching the soft segments, typical of an exfoliated nanocomposite.

to conventional polyurethanes, which is known to be in the region of 80 ± 1° without significantly large contact angle hysteresis.[35] Known causes of a large hysteresis loop include surface roughness, microscale chemical heterogeneity, and surface fabrication in an aqueous environment. All samples were dried and cast in a hot air oven at 70 °C, which excludes an aqueous environment. TEM studies showed chemical heterogeneity; then, the advanced angle is thought to be typical of the low-energy surface component and the receded angle typical of the high-energy surface component. As such, AFM was performed to determine if there was a significant topographic contribution.

Surface Topography. Atomic force microscopy in contact mode shows that 2% POSS−PCU has three different phases: a crystalline-like phase and a two-phase "pebble−stone" blend. The smooth crystalline phase consist of domains that are 5−20 μm in size with a height of 1−6 μm compared to base level (Figure 4A). The pebble−stone blend can only be observed at higher magnifications (Figure 4B) and consists of elevated domains that are 200−500 nm in size and 100−200 nm in

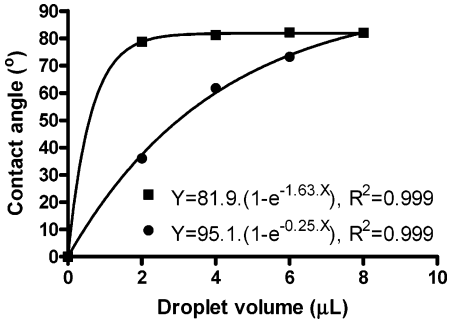

Figure 3. Large contact angle hysteresis loop of 2% POSS−PCU nanocomposites. (■), advancing; (●), receding.

height. The friction image (right figure in Figure 4B) shows that the elevations and depressions have different viscoelastic properties[53] and therefore can be considered as two separate phases. A friction image maps the twisting of the cantilever that arises from forces on the AFM cantilever parallel to the plane of the sample surface. Further images were obtained in intermittent contact mode from transition zones between elevations and depressions. In intermittent contact mode, the phase image shows the relative adhesion between the tip and the sample, in addition to height information. The depressions have a lower adhesion compared to the elevations and therefore appear darker in Figure 4C. This figure also shows the presence of transitional intercalating zones with an intermediate adhesion compared to the other domains. This is in contrast to the PCU control, which shows the diminished presence of a crystalline phase and the absence of a two-phase pebble−stone blend (Figure 4D).

Thromboelastography. TEG is a sensitive indicator of thrombogenicity, and we used these as screening tests to ascertain the antithrombogenic properties of POSS−PCU. We found that the polymer had a lower maximum amplitude (MA) value(s) indicative of decreased platelet bonding strength ($p < 0.001$, one-way ANOVA) as compared to control polystyrene and PCU. In addition, it was also found that the clots which formed on POSS−PCU were significantly unstable and lysed by 60 min compared to PCU or the control polystyrene polymer ($p < 0.0001$, 0ne-way ANOVA). Both MA and LY60 results are shown in Figure 5. These results may be due to either decreased fibrin binding strength to the polymer or lower fibrin adsorption to the TEG cup or a combination of both. In the following series of experiments, we sought to determine the cause of this behavior. As mentioned earlier, these tests were not performed with PTFE and poly(ethylene terephthalate), as it is not possible to evenly coat onto the TEG cups as is the case with PCU and POSS−PCU, since PTFE and Dacron are high-extrusion-based polymers.

Fibrinogen Adsorption Tests. Direct ELISA fibrinogen adsorption analyses ($n = 4$) to the various polymers showed that there was a significantly decreased fibrinogen adsorption to the polyurethanes (POSS−PCU and PCU) as compared to PTFE ($p < 0.01$, one-way ANOVA analysis) (Figure 6). In the case of POSS−PCU, this may again be attributed to the effect of polyhedral oligomeric silsesquioxane (POSS) groups on the PCU surface, which possess a variable surface tension and hence reduce both platelet and protein adsorption. Although we found no significant difference between POSS−PCU and PCU in terms of fibrinogen adsorption, TEG analyses show that the strength of the fibrin clot in POSS−PCU is much weaker as compared to PCU. This indicated that, while the amounts of fibrinogen adsorbing to both polymers are similar, the binding strength is weaker in POSS−PCU compared to PCU alone. No comparisons were done with poly(ethylene terephthalate) for the reasons discussed above.

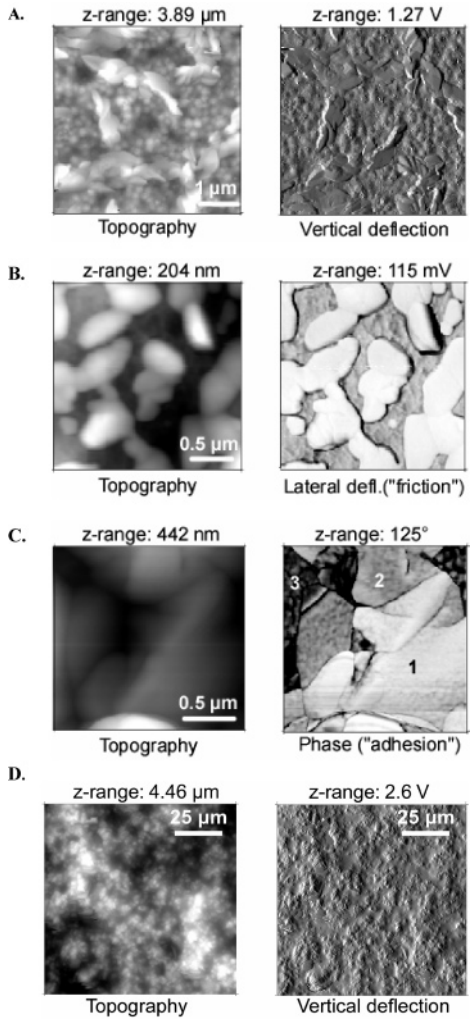

Figure 4. (A) Topography (left) and vertical deflection image (right) obtained in contact mode of 2% POSS−PCU showing the crystalline-like phase that consists of domains of 5−20 μm in size and 1−6 μm in height relative to the binary mixture phase. (B) Topography (left) and friction image (right) obtained in contact mode of a 2.3 × 2.3 μm^2 area of 2% POSS−PCU showing a two-phase pebble−stone blend consisting of elevated domains that are 200−500 nm in size and 100−200 nm in height. The friction image (right) maps the lateral deflection (twisting) of the cantilever that arises from forces on the AFM cantilever parallel to the plane of the sample surface. This image shows that the elevations and the depressions have different viscoelastic properties and therefore can be considered two separate phases. (C) Topography (left) and phase image (right) obtained in intermittent contact mode of 2% POSS−PCU showing the transition zone between elevations and depressions in the two-phase pebble−stone blend. The depressions (3) have a lower adhesion compared to the elevations (1) and therefore appear darker in part C. This figure shows the presence of transitional intercalating zones (2) with intermediate adhesion compared to the two other domains. (D) Surface topography of the control PCU.

Antifactor Xa Activity. Factor X is a crucial element of both the intrinsic and extrinsic coagulation pathways. Using the methods described earlier, we first compared the surface anti-FXa activity of 2% POSS−PCU to PCU and PTFE. On increasing the concentrations of POSS in PCU to 2% and then 6%, we found a proportionate increase in the anti-FXa activity of the copolymer as compared to both PCU and PTFE (Figure 7), which was statistically very significant (one-way ANOVA, $p < 0.0001$). These findings indicate that POSS−PCU nano-

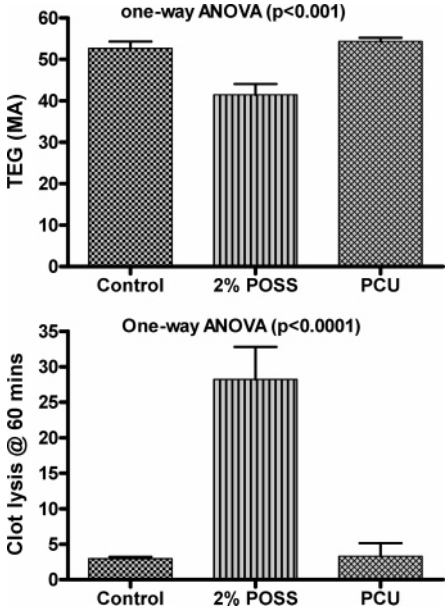

Figure 5. Tests showing lower maximum TEG amplitude (MA) values and increased clot lysis at 60 min of 2% POSS−PCU compared to PCU and the polystyrene control ($n = 6$).

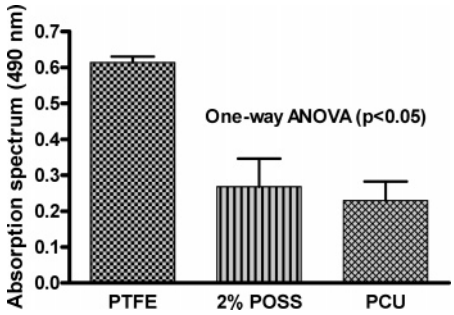

Figure 6. Fibrinogen adsorption direct ELISA tests on 2% POSS−PCU, PCU, and PTFE ($n = 4$).

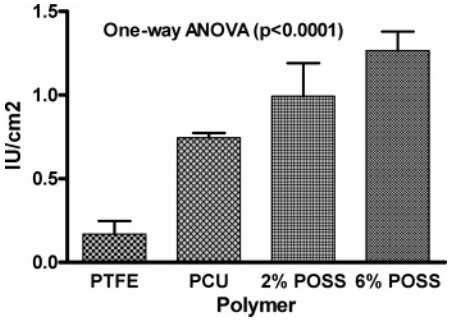

Figure 7. Incremental concentrations of POSS within PCU conferring greater anti-FXa activity ($n = 6$).

composites inactivate FXa to a greater extent than PTFE and PCU. It is important to note that PCU also exhibited some, if not as significant, FXa inactivation. Correlating this with the AFM data suggests that increasing the nanoscale surface roughness of the polymer would enhance FXa denaturation and inactivation.[36] Since we are primarily interested in graft material for smaller-diameter (<6 mm) and microvessels (<1 mm), no tests on poly(ethylene terephthalate) were performed. It must be mentioned here that 2% POSS−PCU gained precedence over 6% POSS−PCU as a vascular graft, since the latter was markedly stiffer during radial compliance studies.

Platelet Adsorption Test. Platelet adsorption onto cast sheets of POSS−PCU was significantly less than both PCU and PTFE

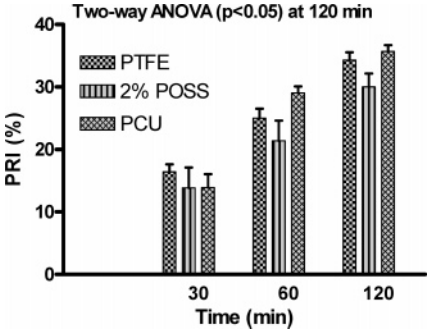

Figure 8. Platelet retention indices (PRI) on 2% POSS−PCU, PCU, and PTFE at 30, 60, and 120 min ($n = 6$) showing significant decrease in platelet adsorption to 2% POSS−PCU compared to PCU and PTFE.

sheets in vitro after 120 min in contact. Statistical analysis using two-way ANOVA showed significant difference (two-way ANOVA, $p < 0.05$) in platelet adsorption by 120 min between POSS−PCU, PCU, and PTFE, as shown in Figure 8. These results indicate that POSS−PCU repels platelet adsorption with increasing time to its surface to a greater extent compared to PTFE and PCU. In conjunction with the lower MA values obtained on TEG, this suggests that POSS−PCU has an anti-platelet effect by both repelling their surface adsorption and lowering the binding strength of platelets to the polymer which correspond to the poor adsorption characteristics exhibited toward fibrinogen discussed above.

SEM analysis performed on these samples at 120 min to assess platelet adsorption morphology revealed very few platelets adhering to POSS−PCU (Figure 9B) compared to the uniform, thick layer of platelets deposited on PTFE as shown in Figure 9A. These images supported the PRI studies conducted on polymer−platelet adhesion which showed decrease adhesion to the nanocomposite.

Platelet adsorption patterns were then graded on the basis of Cooper's arbitrary classification scheme (Table 1).[37] According to this scheme, there was minimal platelet adsorption to certain areas, which corresponds to the POSS-rich hard segments, and even those platelets that did adsorb showed stage I patterns: round platelets with no pseudopodia. Platelet adsorption to the remaining regions was greater in comparison with Cooper stage II type adsorption patterns: rounded platelets with early pseudopodia present, indicating moderate adsorption, probably to the soft segment. In contrast, platelet adsorption to PTFE was far greater with multiple layers of adherent platelets visualized even at lower magnifications. These platelets exhibited stage IV adsorption patterns in over 50% of the surface area. These findings show that integrin activation on platelets[26] occurs to a lesser extent in POSS nanocomposites as compared to PTFE. This improved haemocompatibility corroborates with previous studies on silicon-containing polymers.[17] Platelet adsorption tests on Dacron were not performed, since they are known to possess relatively high platelet adsorption characteristics,[3] even significantly higher than PTFE.

Discussion

It is well-documented that silicon polymers have variable surface tensions which confer both anti-protein and anti-platelet actions.[17] In the past, incorporation of silicon into copolymers has been in the form of siloxane, which in itself is noncompliant with low patency rates[38] as a result of elasticity mismatch causing intimal hyperplasia.[9,14] Methods have been afoot to

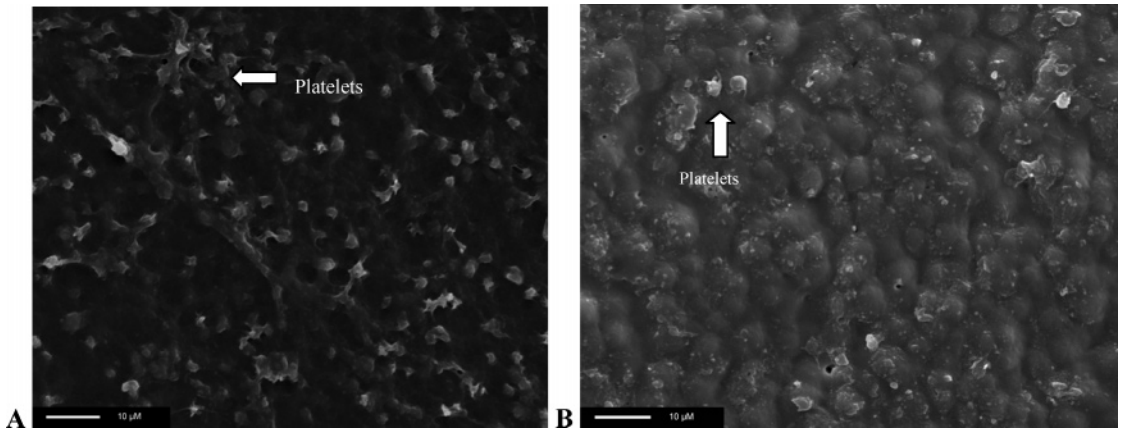

Figure 9. SEM images of platelet adsorption. (A) Uniform platelet adsorption on PTFE (stage IV) after incubation for 120 min. (B) Platelet adsorption on 2% POSS−PCU showing minimal platelet adsorption at 120 min (stage I) with the white specks of platelets marked with the pebblestone background of POSS−PCU in the background. Magnification at 1250×.

Table 1. Cooper's Classification Scheme for Platelet Adsorption[37]

stage	description
I	rounded platelets with no pseudopodia.
II	dendritic, rounded platelets with early pseudopodia formation.
III	spreading, dendritic platelets.
IV	spreading platelets and their hyaloplasms with prominent pseudopodial formation.
V	fully spread platelets over the entire surface.

preserve the surface properties of silicon by combining it with more compliant polymers such as rubber,[39] but results have been suboptimal. An alternative would be incorporating silicon in the form of nanoscale POSS molecules as side-chain groups,[19,40] which would preserve compliance of the copolymer while further lowering its surface tension properties, as nanocomposites have been shown to result in values of less than 20 mJ/m.[41,42] These results are even lower than those for fluorinated PTFE molecule, the current biomaterial(s) of choice for small diameter[43] and microvascular grafts. A further advantage is that, as experiments on dental materials have shown, this variable surface tension could also mean lower bacterial adhesion, thus creating an antibacterial surface action as well.[44,45]

The factors which determine particle adsorption to a polymeric interface are (1) surface tension, (2) surface morphology/configuration, and (3) particle size. The surface tension so often confused with hydrophobicity[46] is defined as the amount of work required to increase the surface area of a substance by 1 cm^2 and is a measure of its surface reactivity. For instance, air has a low surface tension, while water possesses high surface tension values.[47] These measurements involve analyzing the static and dynamic contact angles of surfaces using a variety of liquids.[48] Monte Carlo simulation studies have shown that hydrophobic surfaces are better at repelling larger particles, and vice versa for hydrophilic ones. These researchers have also proven that polymers with extended surface configurations wherein the monomeric units overlap one another have lower particle adsorption, particularly for larger-sized molecules such as proteins.[49] With respect to haemocompatibility, the primary proteins in question are fibrinogen and the coagulating proteins.

In the past, Feng and co-workers showed that the haemocompatibility of low-temperature isotope carbon (LTIC) is greater than that of conventional silicone polymers, as it denatures or alters the conformation of adsorbed fibrinogen to a greater extent.[50] Our contact angle measurements however indicate that, unlike earlier silicones,[35] POSS−PCU based nanocomposites possess large contact angle hysteresis, which has been shown to affect the conformation of particles such as fibrinogen adsorbed to its surface.[51] Subsequent tests showed that fibrinogen also had decreased quantitative and qualitative adsorption to POSS−PCU surfaces as exemplified by direct ELISA and TEG, respectively. While there was no significant difference in fibrinogen adsorption between PCU and POSS−PCU, there exists a marked difference in clot lysis times ($p < 0.01$) between the two polymers. This indicated that, although the number of adsorbed fibrin molecules is similar in quantity, their binding strength to the nanocomposite is much lower, possibly due to a conformational change in adsorbed proteins over time. Studies are currently underway to quantify the degree of conformational change utilizing ellipsometry and small-angle neutron scattering. This may also explain the lower platelet adsorption and maximum amplitude (MA) values to the POSS−PCU as compared to PCU, because platelet adsorption requires a stable configuration of fibrinogen formation.[52,53]

Using polyurethaneureas based on 4,4′-diphenylmethane diisocyanate and polytetramethylene glycols, Groth and co-workers had reported that platelet and protein adsorption increases proportionately with urethane and urea concentrations[26] within the hard segments. This study shows that platelet and protein adsorption to the POSS−PCU nanocomposite was low in all regions including the crystalline segment. This is corroborated by the undulating platelet adsorption topography and the evidence of low-grade platelet adsorption (Cooper grades I) to the nanocomposite that was observed with SEM. This reversal is attributable to the presence of silicon-rich POSS nanocages occupying the hard segment of the nanocomposite and concurrently replacing both urethane and urea and so reducing its concentration.

While the protein-/platelet-repellent nature of this nanocomposite is due to its high contact angle hysteresis, the cause for the degree of hysteresis can be attributed to either its nanoscale chemical heterogeneity and/or its surface topography. TEM and EDXA analyses reveal the heterogeneous nature of the polymer surface at the nanoscale with the POSS nanocages preferentially residing within the hard segments of the nanocomposite with extensions to the soft segment as well. On the basis of X-ray photoelectron spectroscopy (XPS) analyses on silicon−germanium nanocomposites, Muller and co-workers believed that nanoscale surface roughness or topography was the prime factor responsible for this hysteresis[54] as compared to surface composition. On the basis of this background, we performed XPS analyses on 2% and 6% POSS−PCU wherein there was an increase in elemental surface silicon content from 16% to 18%.

Interestingly, there was no difference in contact angle hysteresis between the two nanocomposites, suggesting that surface topography due to the POSS-induced surface reorientation was the main determinant of contact angle hysteresis in this case.

Surface topography may be broadly classified into the mushroom, brush, or pancake profiles.[55] The former two varieties have extended configurations wherein they rise out of the surface, whereas pancake-type profiles have collapsed or flattened surfaces with the highest monomer density within two lattice spaces of the surface. Extended surfaces can extend up to ten lattice spaces (a lattice space may be defined as the space bounded by atoms/molecules with identical surroundings to one another) from the surface with the self-attractive hydrophobic constituents closer to the surface and the hydrophilic constituents further away from the surface,[49] the degree to which depends on the nature of the contacting surface. Monte Carlo simulation studies indicate that polymers with extended configurations would repel particle adsorption better than collapsed ones as long as the ratio of particle size to polymer layer is four or greater.[56] This strengthens the argument for the inclusion of nanofillers onto interfaces in contact with large molecules such as proteins. The use of such nanomaterials would increase this ratio significantly and so improve protein repulsion and, in the case of blood, platelets as well. Interestingly, such nanoengineered surfaces would be more able to adsorb very small particles[49] such as low molecular weight heparin while repelling the larger coagulant proteins, making them ideal at the vascular interface. In this case, the extremely small size of silicon in the form of POSS nanocages (1−3 nm)[57] would further increase the ratio of particle size to polymer layer and thereby accentuate both platelet and protein repulsion.

Intermittent contact mode AFM studies on these POSS−PCU nanocomposites revealed a nanoscale extended surface configuration with a "mushroom/domelike" profile. Its surface nanoarchitecture is such that POSS-rich hard segments were found to reside closer to the surface as depressions, while the more hydrophilic soft segments rise from the surface as elevations, which is in keeping with existing data on polymers possessing both hydrophobic and hydrophilic elements[49] being amphiphilic in nature. The lower adhesion exhibited between the contact probe of the AFM and the darker, depressed areas also corresponded to the decreased platelet and protein adsorption behavior on SEM to the depressed areas of the nanocomposite, while the brighter, elevated regions show relatively higher adhesion characteristics.

As a significant proportion of this POSS−PCU nanocomposite surface consists of peaks at the microscale and domes at the nanoscale, it would be not be wrong to expect increased overall surface protein adsorption. In contrast, quite the opposite is true. Similar studies on globulin[54] and macrophage[36] using silicone−germanium nanocomposites had shown that, although these so-called peaks or "nanopyramids"[36] exhibited increased protein adsorption, the adsorbed proteins were actually inactive, as this nanoscale roughness contributes to large contact angle hysteresis.[54] This would also explain why FXa inhibition is present, although to a lesser extent, in the control polymer (PCU), as it showed microscale surface roughness on AFM studies. Interestingly, there is a proportionate increase in FXa inhibition on increasing POSS nanocage concentrations, as this would increase surface nanostructure density and contact angle hysteresis further, which would in turn accelerate protein denaturation.

While we agree with previous work that this antithrombogenic effect is a result of the surface morphology of nanocomposites, AFM experiments on these POSS−PCU nanocomposites and the PCU controls also reveal that the addition of nanofillers is necessary in creating these nanostructures in the first place. In all, both surface composition and morphology are a must in order to elicit this protein-repellent activity.

Assays to show irreversible protein adsorption to the polymers were not performed as we felt that testing them in a dynamic setting using pulsatile flow was more physiological. These tests are currently underway as further investigations on these nanomaterials are performed in addition to the surface ellipsometry and small angle neutron scattering studies described earlier. If all our results hold true in vivo, thrombus formation on POSS−PCU would be unstable and weak with a lower propensity for thrombus propagation and vessel occlusion. Animal studies using the rat femoral artery vascular model are also being performed to further confirm this.

This represents the first reported literature of the antithrombogenic effect of POSS−PCU nanocomposites. This group of polymers are only now being commercialized in industry, principally within aerospace-based applications, and has few if any practical biomedical applications as of yet. It not only possesses the anti-platelet and anti-protein effects of existing siloxane copolymers but behaves as a surface anticoagulant as well. POSS-incorporated macro- and microvascular interfaces could remove the necessity to heparinize devices such as the heart-lung machines and artificial capillary beds. This approach could also provide a simpler chemical alternative compared to current methods of improving small-diameter and microvascular graft patency. There even is the possibility of tagging molecules such as nitric oxide (NO)[58] as side chains directly to the POSS nanostructure to enhance its haemocompatibility even further. This particular work is currently underway and, if successful, could open up entire vistas for the use of silicon nanocomposites in medicine, particularly as thromboresistant macro- and microvascular interfaces in vivo.

Encouraged by our results, we have fabricated 2% POSS−PCU both as macro- and microvascular grafts, respectively.[59] As far as vessel fabrication is concerned, the ability of POSS to self-assemble predominantly on the surface would mean that the bulk of the polymer would consist of polyurethane molecules cross-linked by POSS nanocages, which preserves radial elasticity and enhances its resistance to degradation.[13,60] This could be a further advantage of POSS−PCU nanocomposites. From the manufacturing point of view, polyurethanes, being low-extrusion polymers, remain as stable liquids with the ability of either dip-coating or extruding them into prostheses. These are still early days to comment on the clinical success of these nanomaterials, but for certain, the future is very bright.

Acknowledgment. We would like to acknowledge the financial support for development of nanomaterials for medical devices provided by UCL BioMedica PLC & EPSRC. H.J.S. would like to thank the trustees of the Royal Free Hampstead NHS Trust Hospital for a Peter Samuel grant for establishing the Advanced Nanomaterials laboratory facility.

References and Notes

(1) Conte, M. S. *FASEB J.* **1998**, *12*, 43−45.
(2) Kannan, R. Y.; Salacinski, H. J.; Butler, P. E.; Hamilton, G.; Seifalian, A. M. *J. Biomed. Mater. Res., Part B* **2005**, *74*, 570−581.
(3) Desai, N. P.; Hubbell, J. A. *J. Biomed. Mater. Res.* **1991**, *25*, 829−843.
(4) Schmedlen, R. H.; Elbjeirami, W. M.; Gobin, A. S.; West, J. L. *Clin. Plast. Surg.* **2003**, *30*, 507−517.
(5) Balasubramanian, V.; Grusin, N. K.; Bucher, R. W.; Turitto, V. T.; Slack, S. M. *J. Biomed. Mater. Res.* **1999**, *44*, 253−260.

(6) Lin, P. H.; Bush, R. L.; Yao, Q.; Lumsden, A. B.; Chen, C. *J. Surg. Res.* **2004**, *118*, 45−52.
(7) Ballyk, P. D.; Walsh, C.; Butany, J.; Ojha, M. *J. Biomech.* **1998**, *31*, 229−237.
(8) Perktold, K.; Leuprecht, A.; Prosi, M.; Berk, T.; Czerny, M.; Trubel, W.; Schima, H. *Ann. Biomed. Eng.* **2002**, *30*, 447−460.
(9) Tai, N. R.; Salacinski, H. J.; Edwards, A.; Hamilton, G.; Seifalian, A. M. *Br. J. Surg.* **2000**, *87*, 1516−1524.
(10) L'Heureux, N.; Paquet, S.; Labbe, R.; Germain, L.; Auger, F. A. *FASEB J.* **1998**, *12*, 47−56.
(11) Baguneid, M.; Murray, D.; Salacinski, H. J.; Fuller, B.; Hamilton, G.; Walker, M.; Seifalian, A. M. *Biotechnol. Appl. Biochem.* **2004**, *39*, 151−157.
(12) Lelah, M. D.; Cooper, S. L. *Polyurethanes in medicine*; CRC Press: Boca Raton, FL, 1986.
(13) Salacinski, H. J.; Tai, N. R.; Carson, R. J.; Edwards, A.; Hamilton, G.; Seifalian, A. M. *J. Biomed. Mater. Res.* **2002**, *59*, 207−218.
(14) Seifalian, A. M.; Salacinski, H. J.; Tiwari, A.; Edwards, A.; Bowald, S.; Hamilton, G. *Biomaterials* **2003**, *24*, 2549−2557.
(15) Wetzels G. M.; Koole L. H. *Biomaterials* **1999**, *20*, 1879−1887.
(16) Silver, J. H.; Hergenrother, R. W.; Lin, J. C.; Lim, F.; Lin, H. B.; Okada, T.; Chaudhury, M. K.; Cooper, S. L. *J. Biomed. Mater. Res.* **1995**, *29*, 535−548.
(17) Silver, J. H.; Lin, J. C.; Lim, F.; Tegoulia, V. A.; Chaudhury, M. K.; Cooper, S. L. *Biomaterials* **1999**, *20*, 1533−1543.
(18) Park, J. H.; Bae, Y. H. *Biomaterials* **2002**, *23*, 1797−1808.
(19) Kannan, R. Y.; Salacinski, H. J.; Butler, P. E.; Seifalian, A. M. *Acc. Chem. Res.* In press.
(20) Punshon, G.; Vara, D. S.; Sales, K. M.; Kidane, A. G.; Salacinski, H. J.; Seifalian, A. M. *Biomaterials* **2005**, *26*, 6271−6279.
(21) Fukushit, K.; Sato, T. *Environ. Sci. Technol.* **2005**, *39*, 1250−1256.
(22) Salacinski, H. J.; Handcock, S.; Seifalian, A. M. WO Patent WO2005070998, 2005; http://v3.espacenet.com/textdoc?DB=EPODOC&IDX=WO2005070998&F=0.
(23) Sanchez, C.; Soler-Illia, G. J.; Ribot, F.; Lalot, T.; Mayer, C. R.; Cabuil, V. *Chem. Mater.* **2001**, *2001*, 3061−3083.
(24) Kannan, R. Y.; Salacinski, H. J.; Sales K. M.; Butler, P. E.; Seifalian, A. M. *Cell Biochem. Biophys.* In press.
(25) Lee, Y. J.; Kuo, S. W.; Huang, W. J.; Lee, H. Y.; Chang, F. C. *J. Polym. Sci., Part B: Polym. Phys.* **2004**, *42*, 1127−1136.
(26) Groth, T.; Campbell, E. J.; Herrmann, K.; Seifert, B. *Biomaterials* **1995**, *16*, 1009−1015.
(27) Kannan, R. Y.; Salacinski, H. J.; Ghanavi, J.; Narula, A.; Odlyha, M.; Pairovi, H.; Butler, P. E.; Seifalian, A. M. *Plast. Reconstr. Surg.* In press.
(28) Kim, K.; Yu, M.; Zong, X.; Chiu, J.; Fang, D.; Seo, Y. S.; Hsiao, B. S.; Chu, B.; Hadjiargyrou, M. *Biomaterials* **2003**, *24*, 4977−4985.
(29) Kidane, A. G.; Salacinski, H. J.; Punshon, G.; Ramesh, B.; Srai, K. S.; Seifalian, A. M. *Med. Biol. Eng. Comput.* **2003**, *41*, 740−745.
(30) Kidane, A. G.; Salacinski, H.; Tiwari, A.; Bruckdorfer, K. R.; Seifalian, A. M. *Biomacromolecules* **2004**, *5*, 798−813.
(31) Williams, R. L.; Wilson, D. J.; Rhodes, N. P. *Biomaterials* **2004**, *25*, 4659−4673.
(32) Saito, N.; Nojiri, C.; Kuroda, S.; Sakai, K. *Biomaterials* **1997**, *18*, 1195−1197.
(33) Salzman, E. W. *J. Lab. Clin. Med.* **1963**, *62*, 274.
(34) Novak, B. *Adv. Mater.* **1993**, *5*, 422.
(35) Wang, F. Poly(dimethylsiloxane) Modification of Segmented Thermoplastic Polyurethanes and Polyureas. State University of Virginia, 1998.
(36) Riedel, M.; Muller, B.; Wintermantel, E. *Biomaterials* **2001**, *22*, 2307−2316.
(37) Ko, T. M.; Lin, J. C.; Cooper, S. L. *Biomaterials* **1993**, *14*, 657−664.
(38) Berman, D. E.; Lineweaver, W.; Vasconez, B.; Buncke, H. *Microsurgery* **1986**, *7*, 132−134.
(39) White, R. A.; Klein, S. R.; Shors, E. C. *J. Cardiovasc. Surg.* **1987**, *28*, 485−490.
(40) Nishino, T.; Urushihara, Y.; Meguro, M.; Nakamae, K. *J. Colloid Interface Sci.* **2004**, *279*, 364−369.
(41) Schmidt, H. *Appl. Organomet. Chem.* **2001**, *15*, 331−343.
(42) Schidmt, H.; Kasemann, R.; Burkhart, T.; Wagner, G.; Arpac, E.; Geiter, E. *ACS Symp. Ser.* **1995**, *585*, 331−347.
(43) Nishino, T.; Meguro, M.; Nakamae, K. *Int. J. Adhes. Adhes.* **1999**, *19*, 399−403.
(44) Quirynein, M.; Bollen, C. M. L. *J. Clin. Periodontol.* **1995**, *22*, 1−14.
(45) Knorr, S. D.; Combe, E. C.; Wolff, L. F.; Hodges, J. S. *Dent. Mater.* **2005**, *21*, 272−277.
(46) Blunden, R. E.; Oliver, R. G.; O'Kane, C. O. *Br. J. Orthod.* **1994**, *21*, 125−132.
(47) Nagasawa, A.; Kitano, T.; Watanabe, T.; Fujisawa, K. *Sen'i Gakkaishi* **2004**, *60*, 183−187.
(48) Gu, G. T.; Zhang, Z. J.; Dang, H. X. *Acta Polym. Sin.* **2002**, *6*, 770−774.
(49) Jonsson, M.; Johansson, H. O. *Colloids Surf., B* **2004**, *37*, 71−81.
(50) Feng, L.; Andrade, J. D. *J. Biomed. Mater. Res.* **1994**, *28*, 735−743.
(51) Tengvall, P.; Askendal, A.; Lundstrom, I. *Biomaterials* **1998**, *19*, 935−940.
(52) Hynes, R. O. *Thromb. Haemostasis* **1991**, *66*, 40−43.
(53) Sixma, J. J.; Hindriks, G.; Van Breugel, H.; Hantgan, R.; de Groot, P. G. *J. Biomater. Sci. Polym. Ed.* **1991**, *3*, 17−26.
(54) Muller, B.; Riedel, M.; Michel, R.; De Paul, S. M.; Hofer, R.; Heger, D.; Grutzmacher, D. *J. Vac. Sci. Technol., B* **2001**, 19.5, 1715−1720.
(55) Fleer, G. J.; Cohen Stuart, M. A.; Scheutjens, J. M. H. M.; Cosgrove, T.; Vincent, B. *Polymers at interfaces*, 1st ed.; Chapman & Hall: London, 1993.
(56) Malmsten, M.; Burns, N.; Veide, A. *J. Colloid Interface Sci.* **1998**, *204*, 104−111.
(57) Xiang, K.; Pandey, R.; Pernisz, U. C.; Freeman, C. *J. Phys. Chem. B* **1998**, *102*, 8704.
(58) Duan, X.; Lewis, R. S. *Biomaterials* **2002**, *23*, 1197−1203.
(59) Kannan, R. Y.; Salacinski, H. J.; Sales, K.; Butler, P.; Seifalian, A. M. *Biomaterials* **2005**, *26*, 1857−1875.
(60) Kannan, R. Y.; Salacinski, H. J.; Odlyha, M.; Butler, P. E.; Seifalian, A. M. *Biomaterials* In press.

BM050590Z